Mol Neurobiol (2017) 54:1939–1952
DOI 10.1007/s12035-016-9783-8

A Novel, Multi-Target Natural Drug Candidate, Matrine, Improves Cognitive Deficits in Alzheimer's Disease Transgenic Mice by Inhibiting Aβ Aggregation and Blocking the RAGE/Aβ Axis

Lili Cui[1] · Yujie Cai[1] · Wanwen Cheng[1] · Gen Liu[1] · Jianghao Zhao[1,2] · Hao Cao[3] · Hua Tao[1,2] · Yan Wang[4] · Mingkang Yin[1] · Tingting Liu[1] · Yu Liu[1] · Pengru Huang[1] · Zhou Liu[1] · Keshen Li[1,5] · Bin Zhao[1]

Received: 9 September 2015 / Accepted: 8 February 2016 / Published online: 22 February 2016

Abstract The treatment of AD is a topic that has puzzled researchers for many years. Current mainstream theories still consider Aβ to be the most important target for the cure of AD. In this study, we attempted to explore multiple targets for AD treatments with the aim of identifying a qualified compound that could both inhibit the aggregation of Aβ and block the RAGE/Aβ axis. We believed that a compound that targets both Aβ and RAGE may be a feasible strategy for AD treatment. A novel and small natural compound, Matrine (Mat), was identified by high-throughput screening of the main components of traditional Chinese herbs used to treat dementia. Various experimental techniques were used to evaluate the effect of Mat on these two targets both in vitro and in AD mouse model. Mat could inhibit Aβ42-induced cytotoxicity and suppress the Aβ/RAGE signaling pathway in vitro. Additionally, the results of in vivo evaluations of the effects of Mat on the two targets were consistent with the results of our in vitro studies. Furthermore, Mat reduced proinflammatory cytokines and Aβ deposition and attenuated the memory deficits of AD transgenic mice. We believe that this novel, multi-target strategy to inhibit both Aβ and RAGE, is worthy of further exploration. Therefore, our future studies will focus on identifying even more effective multi-target compounds for the treatment of AD based on the molecular structure of Mat.

Keywords Matrine · Alzheimer's disease · Receptors for Advanced glycation end product · β-Amyloid peptide

Lili Cui, Yujie Cai and Wanwen Cheng contributed equally to this work.

✉ Lili Cui
lilicui_gmu@163.com

✉ Keshen Li
lilicui_gmu@163.com

✉ Bin Zhao
binzhao0759@163.com

[1] Guangdong key laboratory of age-related cardiac and cerebral diseases, Affiliated Hospital of Guangdong Medical University, Zhanjiang, Guangdong Province, China

[2] Institutes of Neurology, Affiliated Hospital of Guangdong Medical University, Zhanjiang, People's Republic of China

[3] Departments of Life Science and Biopharmaceutics, Shenyang Pharmaceutical University, Shenyang, China

[4] Clinical Research Center, Affiliated Hospital of Guangdong Medical University, Zhanjiang, People's Republic of China

[5] Institute of clinical medicine, Jinan University, Guangzhou, People's Republic of China

Introduction

Alzheimer's disease (AD) is a progressive neurodegenerative disorder that affects the elderly. Abnormal accumulation of β amyloid peptide (Aβ) results in insignificant neurotoxicity in the nervous system, and this neurotoxicity is recognized as one of the most important hallmarks of AD and the underlying pathological processes [1–3]. Aβ is generated through the sequential proteolytic processing of amyloid precursor protein (APP) by β-site APP cleaving enzyme 1 (BACE1) and γ-secretase. The over production or insufficient clearance of Aβ aggregates results in the formation of oligomers to fibrils and amyloid plaques under the pathological conditions of AD, and these aggregates contribute to neuronal deterioration in

AD patients [4–6]. Current research has demonstrated that Aβ aggregation, particularly of Aβ oligomers, is correlated with the degree of cognitive deficits, likely because Aβ oligomers exhibit the greatest neurotoxicity in AD [7, 8]. Therefore, identifying a way to prevent Aβ overproduction or Aβ aggregation, which would help inhibit Aβ-induced neurotoxicity, is a promising avenue for AD therapy [9–12].

Several compounds have been reported that could inhibit Aβ-induced neurotoxicity in vitro and that have been shown to reduce or improve cognitive deficits in a transgenic mouse model of AD [13–19]. Furthermore, Aβ inhibitors that target the key secretase of the APP pathway have also shown potential utility for the treatment of AD [20–24]. However, due to obstacles of the effective use of such drugs, such as the drug delivery method, the blood brain barrier (BBB) and safety, to date, drugs that target the secretases involved in the Aβ and APP pathways have not yet shown encouraging results in clinical trials [25, 26].

Receptor for advanced glycation end products (RAGE) is an important cell surface receptor that contains an extracellular V domain and a C1 domain that can bind multiple ligands, including Aβ. Aβ/RAGE signaling has been reported to perturb the APP pathway and to induce neuroinflammation, ultimately impairing neuronal function and contributing to the pathogenesis of AD [27–30]. Abnormal overexpression of RAGE is found in the hippocampus of AD mice and AD patients, while the severity of AD is also well correlated with the level of RAGE expression [31, 32]. Moreover, Aβ clearance via RAGE-mediated transport across the BBB contributes to the progressive accumulation of Aβ in sporadic AD [33, 34]. All of the AD-related research into RAGE function has suggested that RAGE is a potential new therapeutic target for AD [35–38].

Previous studies led us to believe that focusing on a single target may not be the most effective way to develop an effective AD treatment. Rather, cooperative, multi-target therapy may have more potential [39, 40]. We hypothesized that a compound that targeted both Aβ and RAGE might be a more promising strategy for the treatment of AD. In this study, we screened natural, small-molecule compounds with double targets that could both inhibit the aggregation of Aβ and block the Aβ/RAGE axis. Herein, we report a novel, natural small compound Matrine (Mat), which was identified by a high-throughput screening of the main components of traditional Chinese herbs used to treat dementia. We analyzed the effects of Mat as an inhibitor of Aβ aggregation and a blocker of the Aβ-mediated RAGE signaling pathway in vitro and evaluated the effects of Mat over a 30-day treatment course in the APP/PS1 double transgenic mouse model of AD in an attempt to explore the treatment of AD multi-target drugs.

Materials and Methods

Preparation of Aβ42 Aggregates

Human Aβ42 was purchased from Sigma-Aldrich (St. Louis, MO, USA). Aβ42 was dissolved in 1,1,1,3,3,3-hexafluoro-2-propanol (HFIP) to 1 mg/mL, sonicated in a water bath for 10 min, vacuum-dried, and then dissolved in dimethyl sulfoxide (DMSO, Sangon Biotech, Shanghai, China) to 1 mg/mL. The fresh Aβ42 solutions (Aβ42 monomers) were stored at −80 °C before use.

Cell Culture and MTT Analysis

SH-SY5Y cells (Biowit Technologies, Shenzhen, China) were cultured in DMEM (HyClone, Logan, UT, USA) that was supplemented with 10 % FBS (Gibco, Grand Island, NY, USA), 100 U/ml penicillin G, and 0.1 mg/ml streptomycin (HyClone, Logan, UT, USA) at 37 °C in a humidified incubator (ESCO, Changi, Singapore) containing 5 % CO_2. The cells were grown to 75 % confluence in 96-well cell culture plates. After culturing for 1 day to allow for cell attachment, the cells were treated with 10-μM fresh Aβ42 and Aβ42 oligomers, respectively, adding with 10 μM (low dose) or 50 μM (high dose) Mat (Chengdu Biopurify Phytochemicals Ltd, Sichuan, China) for 12, 24, and 72 h at 37 °C. Cells that did not receive treatment were used as a blank control. Cell viability was determined by measuring cellular redox activity with 3-(4,5-dimethylthiazol-2-yl)-2,5-diphenyltetrazolium bromide (MTT). MTT (10 μL of 5 mg/mL) was added to each well, and the plates were allowed to incubate at 37 °C for 4 h. Then, 150 μL DMSO was added to each well with shaking for 10 min. The assay was quantified using an automatic microplate spectrophotometer (BioTek, Vermont, USA) at 490 nm. Averages from three replicate wells were used for each condition. Cell viability was calculated by dividing the absorbance of wells containing samples by the absorbance of wells containing medium alone (without DMSO) and multiplying by 100 %.

TEM

Mat (50 μM) was incubated with or without 20-μM fresh Aβ42/Aβ42 oligomers for 12, 24, and 72 h at 37 °C. The sample was spotted onto a 230-mesh Formvar-coated copper grid for 30 min and then displaced with an equal volume of 2.5 % (*v*/*v*) glutaraldehyde in water for 5 min. Then, the grids were stained with 10 μL 3 % (*v*/*v*) filtered uranyl acetate that was filtered in water for 3 min. The grids were then dried and examined with a transmission electron microscope (FE-TEM, JEOL JEM-1400, Japan) with an accelerating voltage of 80 kV.

ThT Staining Analysis

Thioflavin T (ThT)-induced fluorescence assay was used to measure Aβ42 formation using a Hitachi F-2500 Spectro Fluorophotometer. Mat (50 μM low dose or 200 μM high dose) was incubated with or without 20-μM Aβ42/Aβ42 oligomers for 12, 24, or 72 h at 37 °C, with the periodic addition of 990 μL of 3 μM ThT in 50-mM phosphate buffer (pH 6.0). Each assay was performed in triplicate, and fluorescence intensities were measured at 450 nm (excitation) and 485 nm (emission) under time-resolved fluorescence mode.

MST Assays

Microscale thermophoresis (MST) is a novel method to detect interactions between proteins or between proteins and small molecules, such as ligands, and this method has been described in detail elsewhere [41, 42]. Interactions between purchased human RAGE protein (Catalog Number: 11629-HCCH, Sino Biological Inc.) and Mat were measured using MST with a Monolith NT.115 (Nano Temper Technologies GmbH). The RAGE protein was labeled with a fluorescent dye (NT-647) using Monolith NT Protein Labeling Kits (amine reactive) according to the manufacturer's protocol. The concentration of the labeled RAGE protein was held constant at 50 nM, while the concentration of Mat was varied between 0.03 and 1000 μM. The assay was performed in MST buffer that contained 50 mM Tris-HCl (pH 7.6), 150 mM NaCl, 10 mM $MgCl_2$, and 0.05 % Tween 20. The samples were loaded into MST NT.115 premium capillaries after they were incubated at room temperature for 10 min. Thermophoresis was measured with 20 % LED power and 40 % infrared laser power, and the data were analyzed using Nano temper Analysis software, v.1.5.41.

Stable Transfection with Lentivirus

The primers for amplification and identification were designed based on the coding sequence of the human RAGE gene in Gene Bank (NCBI Reference Sequence: Chromosome 6-NC_000006.12) using Primer Premier 5.0 software. The primers used were as follows: pLVX-AGER-MluI-F5′-CGGACGCGTGCCACCATGGCAGCCGGAACAG CAGTTGGAGCCTGGGTGC3′, and pLVX-AGER-NotI-R 5′-ATTTGCGGCCGCTCAAGGCCCTC CAGTACTACTCTCGC-3′. The RAGE fragment was amplified by PCR and recovered through agarose gel electrophoresis. Then, the cloning vector pLVX-mCMV-tdTomato-PGK-Puro(Amp^+) and the RAGE fragment were digested with the restriction enzymes Mlu I and Not I, respectively (1215 bp), and then connected to a construct shuttle plasmid using T4 DNA Ligase (New England Biolabs, Ipswich, MA, USA). The products were transformed into JM109 competent cells (Biowit Technologies, Shenzhen, China) that were coated on selective LB plating medium (Amp^+, 100 μg/ml). Selected monoclonal colonies were identified by gene sequencing. The pLVX-RAGE-mCMV-tdTomato-PGK-Puro plasmid was extracted from the colony along with the lentiviral packaging mixture. These were then co-transfected into 293T cells (Biowit Technologies Shenzhen, China) to package the rLv-hAGER using the HET kit (Biowit Technologies, Shenzhen, China) according to the manufacturer's instructions. After 24 and 48 h, the supernatant containing the rLv-RAGE was collected, concentrated, and purified. Prior to the transfection experiments, the SH-SY5Y cells were grown to 80 % confluence in 24-well cell culture plates. The next day, the cells were transferred into fresh media that contained 6 μg/ml polybrene and transduction-ready lentiviral particles at a multiplicity of infection (MOI) of 20, which had been determined in preliminary trials. The cells were then washed with phosphate-buffered saline (PBS) and returned to growth media after 24 h. Stable clones were selected from colonies that survived exposure to a titrated lethal dose of puromycin antibiotic after several passages. The transfection efficiency was analyzed by PCR, immunofluorescence, and Western blotting analysis.

Animals and Administration

The APP/PS1 transgenic mice (B6C3-Tg (APPswe, PSEN1dE9) 85Dbo/J) were purchased from the Model Animal Resource center of Nanjing University (Nanjing, China). The mice were housed in a controlled animal facility (22–25 °C, 40–60 % relative humidity) with a 12:12-h light–dark cycle and allowed free access to rodent chow and water. Ten-month-old mice were separated into four groups: high-dose Mat-treated AD mice ($n=4$), low-dose Mat-treated AD mice ($n=4$), AD control mice ($n=4$) and WT control BALB/C mice ($n=4$). The mice in the Mat-treated groups received intraperitoneal (I.P.) injections of a daily dose of 50 (low dose) or 100 mg/kg (high dose) Mat (dissolved in physiological saline) for 4 weeks. The mice in the AD control and WT groups were treated with physiological saline (0.9 %). After the last administration of the 30-day treatment, the mice were trained and tested on the Morris water maze (MWM).

MWM Test

The effect of Mat on the spatial cognition of the AD mice was investigated through the MWM test, including a 5-day place navigation test and a 1-day spatial probe test. The maze (Zhongshidichuang Science and Technology Development Co., Ltd, Beijing, China) consisted of a circular pool (diameter of 120 cm and height of 30 cm) that was filled with antholeucin water (25.0 ± 1.0 °C) and that also contained a white-painted circular platform in the center of one quadrant that was submerged 1 cm below the surface of the water. Each

mouse was given three tests on each day of the 5-day place navigation test. In each test, the mouse was allowed to swim for a maximum of 90 s to find the hidden platform and was then allowed to have a 30-s rest period on it. Mice that were unable to locate the platform within the allotted time period were guided to it. The spatial probe test was accomplished in the pool without the platform and was used to measure the time the mouse spent swimming in the quadrant where the platform had been previously located, for a total of 120 s. The swimming activity of each mouse was monitored and recorded using a video camera and then analyzed by software.

Sample Preparation

At the end of the MWM test, the mice were anesthetized and transcardially perfused with ice-cold saline and 4 % paraformaldehyde and then sacrificed by decapitation. The brains were removed. Half of each brain was fixed overnight and embedded in paraffin for histochemical analysis. The other half was used for the Western blotting and ELISA assays.

Immunohistochemistry and Immunohistochemical Analysis

The embedded brains were sectioned at a thickness of 15 μm in the coronal plane. The coronal paraffin sections were dewaxed, rehydrated, and then treated in citric acid buffer (pH 6.0) in a 95 °C water bath for 20 min to expose the epitope. After the sections were washed three times with PBS (pH 7.4), they were treated with 3 % H_2O_2 for 10 min to quench endogenous peroxidase activity and then incubated with 5 % goat serum for 30 min. The primary antibodies were applied separately, and the sections were incubated overnight at 4 °C. After the excess primary antibody was removed, part of the section was incubated with the secondary antibody (HRP-conjugate goat anti-rabbit IgG) for 1 h followed by DAB staining. After staining, the section was dehydrated, coverslipped, and examined by microscopy. The other part of section was incubated with the fluorescent secondary antibody (DyLight 488-conjugate goat anti-rabbit IgG) in dark place for 1 h, then mounted with antifade solution, and examined by fluorescence microscopy. All sections were processed under the same standardized conditions, and the relative intensity was analyzed by ImageJ software.

Western Blotting

Homogenates of the mouse brains and harvested cells were lysed in RIPA buffer (Solarbio, Beijing, China), which contained protease inhibitor cocktail (Roche Applied Science, Mannheim, Germany), and then centrifuged at 12000*g* for 10 min at 4 °C. The supernatants were collected, and equal amounts of extracted protein were separated by 12 % SDS–PAGE. After immunoblotting the proteins onto PVDF membranes (Millipore, Billerica, MA), the membranes were then blocked with 5 % nonfat milk for 1 h at room temperature and separately incubated with various primary antibodies overnight at 4 °C. The antibodies that were used included the following: rabbit anti-amyloid oligomer (1:2000; Millipore), rabbit anti-RAGE (1:2000; Cell Signaling Technology, Danvers, MA), rabbit anti-BACE1 (1:2000; Abcam, Cambridge, UK), mouse anti-APP (1:2000; Millipore), rabbit anti-NFκB p65 (1:800, Santa Cruz Biotechnology, Santa Cruz, CA), rabbit anti-GAPDH (1:1000; Cell Signaling Technology), and anti-beta-actin (1:2000; Earth, CA, USA). The membranes were washed three times with PBS containing 0.1 % Tween-20 and then incubated for 1 h with the appropriate species-specific horseradish peroxidase (HRP)-conjugated secondary antibody. The immunoreactive membranes were visualized with the Prolight HRP Chemiluminescent Kit (Tiangen, Beijing, China). Exposures were recorded on X-ray film. β-Actin and GAPDH were used as invariant controls. Variations in density between the target protein bands and the control bands were determined using software Image-Pro plus 6.0.

Real-Time PCR Analysis

Total RNA from homogenates of the mouse brains and the harvested cells was isolated using TRIzol (Invitrogen, CA, USA), according to the manufacturer's instructions. Equal amounts of total RNA were treated with DNase I and then reverse transcribed into complementary DNA (cDNA) using the RevertAid First Strand cDNA Synthesis Kit (Thermo, Waltham, MA, USA). The real-time PCR amplification was performed using the SYBR green method on a Light-Cycler 96 system (Roche Applied Science, Laval, Quebec, Canada). Each cDNA sample was tested in triplicate. The cDNA levels for each template were normalized with GAPDH using the $2^{-\Delta\Delta Ct}$ method. The primers included the following: BACE1: sense, TGGAGGGCTTCTACGTTGTCTT, anti-sense, CCTGAACTCATCGTGCACATG; NF-κB: sense, ATCTGCCGAGTGAACCGAAACT, anti-sense, CCAGCCTGG TCCCGTGAAA; and GADPH: sense, ACCCACTCCTCCACCTTTGA, anti-sense, CTGTTGCTGTAGCCAAATTCGT.

ELISA Assay

The Aβ42 levels in the cells and cell secretions were determined using the Human Amyloid beta peptide 1-42 (Aβ1-42) ELISA Kit (Cusabio, Wuhan, China) according to the manufacturer's protocols. Briefly, the cell extracts and the collected DMEM were added to a 96-well ELISA plate and then reacted with appropriate primary antibodies and HRP-conjugated secondary antibodies. 3,3′,5,5′-

Tetramethylbenzidine (TMB) was used as the substrate, and the results were quantified using an automatic micro-plate spectrophotometer at 450 nm. Averages from two replicate wells were used for each sample. All quantitative analyses were performed by the external standard method, producing a standard curve with a correlation coefficient >0.99.

HPLC Analysis

The BALB/C mice were used to determine the efficiency with which Mat crossed the BBB. Mat was administered I.P. at 100 mg/kg. Serum and brain samples were then extracted at 30 min, 1 h, 2 h, and 4 h (four mice for each time point) and processed to determine the concentration of Mat by high-performance liquid chromatography (HPLC). All HPLC analyses were performed on the Bio-Rad Dio Flow HPLC System with the following parameters: The detector was set at 210 nm, the flow rate was set at 1.0 mL/min, the temperature was set at 25 °C, the injection volume was 5 μL, and a Nova-park C18 column (3.9 mm × 150 mm, 4 μm) was used. All quantitative analyses were performed according to the external standard method, using Mat as an analytical standard to produce the standard curve.

Molecular Docking

Docking experiments were performed in the program AutoDock 4.0. The 3D structure of FA was built via the Insight II/Builder program and then solvated with a box of TIP3P water molecules that extended 10 Å from the boundary of any protein atoms. An appropriate number of counter ions were added to neutralize the system, and then the FA was optimized by energy minimization and molecular dynamics simulations. The crystal structures of the Aβ42 monomer (PDB ID: 1Z0Q) and extracellular domain of RAGE (PDB ID: 4LP5) were chosen for the docking study. The structural integrity of each model was visually examined using DS Visualizer 3.1(http://accelrys.com/products/discoverystudio/visualization-download.php) [43].

Statistical Analysis

The data presented in this study were obtained from at least three independent experiments for each experimental condition. The data are expressed as the mean ± the SEM, either Student's *t* test or two-way ANOVA (SPSS, version 14.0). For comparisons between control and experimental results, $*p < 0.05$ and $**p < 0.01$ were considered significant. Multiple comparisons were performed with Duncan's test.

Results

Mat Inhibits the Aβ42-Induced Cytotoxicity by Inhibiting the Aggregation of Aβ42

The effects of Mat on Aβ-induced neurotoxicity were analyzed in vitro and in SH-SY5Y cells. As shown in Fig. 1a, b, the high doses of Mat significantly increased the viability of cells treated with fresh Aβ42 monomers in 24 and 72 h ($p = 0.0236$ and $p = 0.0369$, respectively) and with Aβ42 oligomers in 12, 24, and 72 h ($p = 0.0041$, $p = 0.0018$, and $p = 0.013$, respectively). Then, the ThT fluorescence intensity assay was performed to detect the effect of Mat on Aβ42 aggregation, and the results showed that Mat exhibited an inhibitory effect whether the Aβ start the aggregation from the state of monomers or oligomers (Fig. 1c, d). Furthermore, to investigate the effect of Mat on the aggregation of Aβ42, we observed the status of Aβ aggregation under the destabilizing influence of the small molecule Mat using transmission electron microscopy (TEM). As shown in Fig. 1e, f, Mat (50 μM) remarkably inhibited or changed the aggregation of Aβ from monomers to oligomers or to the final state of fibrils. When Mat was acting on preformed Aβ oligomers, we also observed that Mat inhibited or altered the Aβ state transition from oligomer to fibril (Fig. 1g, h), suggesting that Mat could prevent Aβ42 from aggregating or fibrillating along the typical progression of Aβ42 aggregation. This effect may, therefore, weaken Aβ-induced neurotoxicity.

Mat Suppressed the Aβ/RAGE Signaling Pathway and Bound to the RAGE Protein in Vitro

The RAGE-overexpressing SH-SY5Y cell line was used as a cell model to assess the effect of Mat on the Aβ/RAGE signaling pathway. As shown in Fig. 2a–d, the lentiviral vector carrying the RAGE gene was successfully transfected into the SH-SY5Y cell line, and the western blot assay showed that the RAGE protein were overexpressed in SH-SY5Y cell lines. Then, Aβ42 (5 μM) were added to the culture medium of RAGE overexpressed cells as the ligands of RAGE, and two doses of Mat (10 and 50 μM) were added to evaluate the effect of Mat on RAGE signal activation. The results of western blotting showed that Mat dose-dependently inhibited the elevated expression levels of NF-κB ($p = 0.0374$ and $p = 0.0041$, respectively) and BACE1 ($p = 0.028$ and $p = 0.031$, respectively) (Fig. 2e, f), suggesting the inhibiting effect of Mat on RAGE signal pathway. Furthermore, to determine whether Mat bound to RAGE through a direct interaction, we performed MST experiment to assess the binding affinity between RAGE and Mat. We found that RAGE exhibited moderate binding affinity for Mat (KD = 23923.8 μM) (Fig. 2g). These results suggest that Mat has a binding affinity with RAGE and could inhibit the downstream Aβ/RAGE signal pathway.

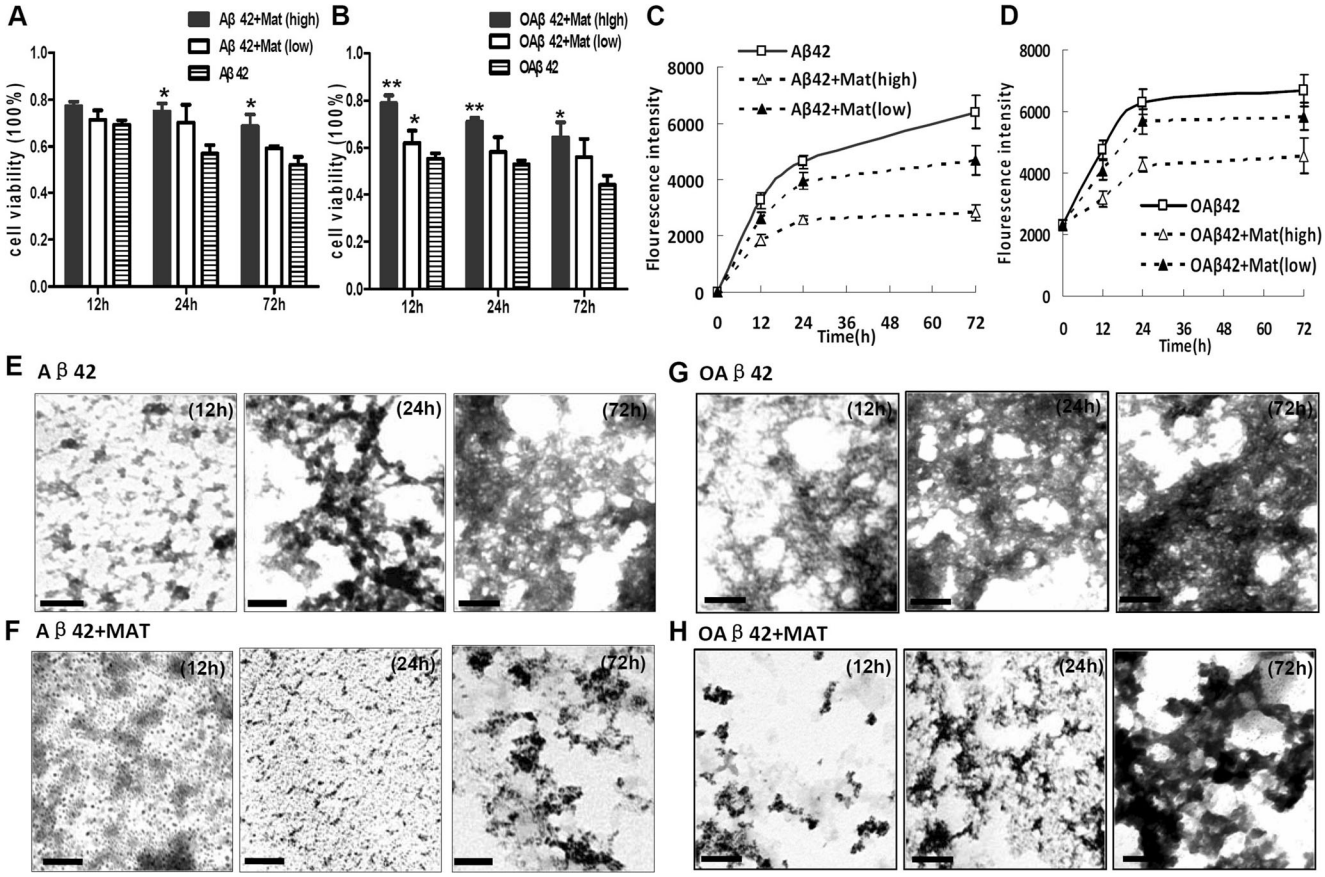

Fig. 1 The effect of Mat on Aβ42 aggregation and Aβ42-induced neurotoxicity. **a** The effects of Mat on Aβ42 monomer-induced neurotoxicity in SH-SY5Y cells. **b** The effect of Mat on Aβ42 oligomer-induced neurotoxicity in SH-SY5Y cells. **c** ThT fluorescence assay-based evaluation of the inhibitory effect of Mat on Aβ42 aggregation. **d** ThT fluorescence assay-based evaluation of the inhibitory effect of Mat on Aβ42 oligomer aggregation. **e**, **f** The influence of Mat on the aggregation of freshly prepared Aβ42 based on TEM observations. **g**, **h** The influence of Mat on Aβ42 oligomer aggregation based on TEM observations. The MTT assay and the ThT fluorescence assays were performed in triplicate. Values are presented as the mean ± SEM; $*p < 0.05$ and $**p < 0.01$, versus Aβ oligomers (oAβ). The TEM images were acquired at 80 kV. The *scale bar* is 100 nm

Mat Attenuates the Memory Deficits of APP/PS1 Transgenic Mice

We further evaluated the effect of Mat on learning and memory in APP/PS1 transgenic mice by the MWM test. Mat was administered to 10-month-old APP/PS1 transgenic mice for 4 weeks and then be tested. As shown in Fig. 3a, compared to the mean escape latency of the control group, the APP/PS1 transgenic mice significantly increased over the 4 days of learning-memory training. Compared with the APP/PS1 transgenic mice, the Mat (high dose)-treated APP/PS1 transgenic mice showed remarkable improvements over the last 2 days of the learning-memory training (Fig. 3b). In the probe trial, the number of platform crossings made by the high dose-treated Mat mice was greater than the number made by the AD mice ($p = 0.0489$). The high dose-treated Mat mice also spent more time in the target quadrant than the AD mice ($p = 0.0321$) (Fig. 3c). The percentage of total distance spent in the target quadrant by the Mat (high dose)-treated APP/PS1 transgenic mice was increased compared to percentage for the control APP/PS1 transgenic mice ($p = 0.0488$) (Fig. 3d). These results suggested that the high dose of Mat significantly improved the memory deficits of the APP/PS1 transgenic mice. However, no significant differences were observed between the Mat (low dose)-treated APP/PS1 transgenic mice and the control APP/PS1 transgenic mice in the above test.

Mat Inhibited the Formation of Senile Plaques and Reduced the Levels of Aβ42 Oligomers in the Hippocampus of APP/PS1 Transgenic Mice

To assess the effect of Mat on Aβ levels in vivo, we investigated the levels of senile plaques and Aβ oligomers in the hippocampus of the AD model mice following the treatment with Mat (high dose). As shown in Fig. 4, the APP/PS1 transgenic mice showed remarkable Aβ plaques in hippocampus compare to Mat-treated AD mice (Fig. 4a, b), and the immunofluorescence assay showed that the Aβ was reduced in the

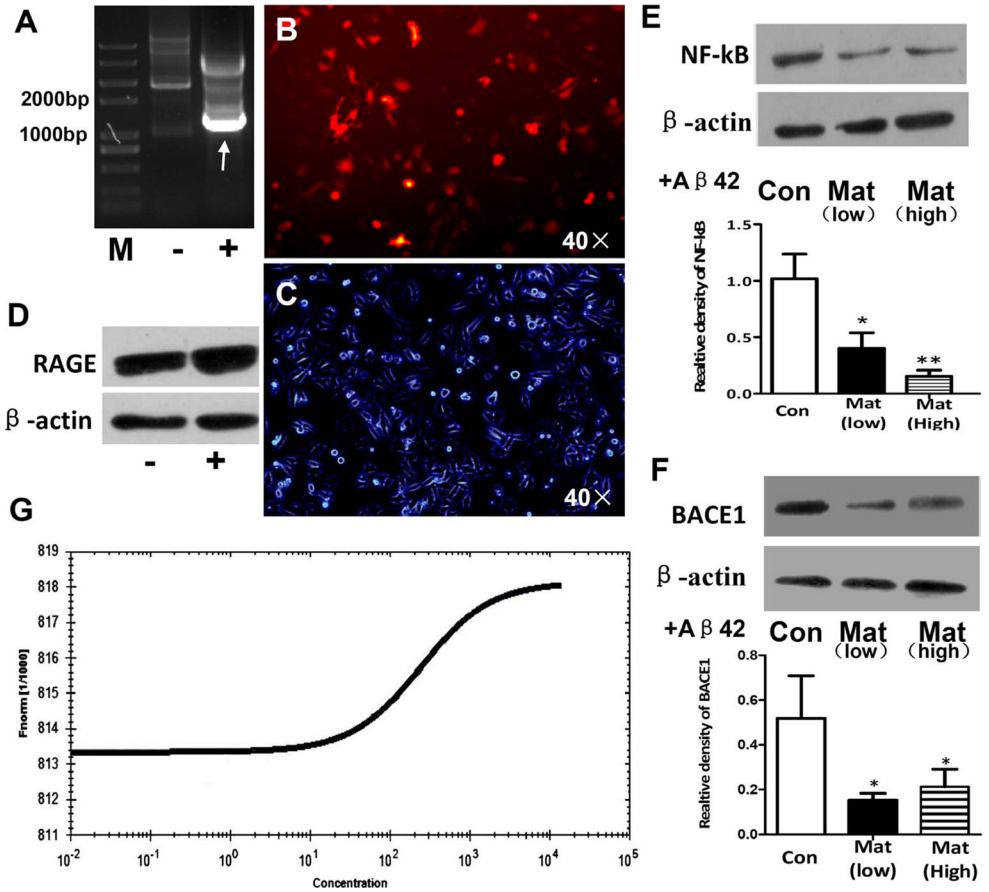

Fig. 2 The effect of Mat-mediated inhibition on the downstream RAGE pathway and the binding affinity between RAGE and Mat. **a** PCR-based identification of the transgenic SH-SY5Y cell line that stably expressed the RAGE gene (1215 bp). *M* indicates the marker, '-' indicates the SH-SY5Y cell line, and '+' indicates the RAGE transgenic SH-SY5Y cell line. **b** Immunofluorescence assay using anti-RAGE antibodies in the RAGE overexpressing SH-SY5Y cell line. **c** Brightfield image of the RAGE overexpressing SH-SY5Y cell line. **d** Western blotting assay for the RAGE protein in the RAGE transgenic SH-SY5Y cell line. **e**, **f** Western blotting assay for NF-κB (**e**) and BACE1 (**f**) with the treatment with the low and high doses of Mat under Aβ stimulation in RAGE-overexpressing cell line. The data are the mean ± SEM; $*p < 0.05$ and $**p < 0.05$, versus the control RAGE transgenic SH-SY5Y cell line

brain of Mat-treated AD mouse than the control APP/PS1 transgenic mice (Fig. 4c, d), and the relative plaque burden area assay showed that Mat could reduce Aβ plaques by 53.89 % (Fig. 4e). Moreover, using the anti-Aβ oligomer antibody, western blotting assay showed that the Mat-treated mice showed lower level of Aβ oligomers ($p = 0.0354$) (Fig. 4f), and the ELISA analysis also revealed that the level of soluble Aβ was reduced after the Mat treatment ($p = 0.0003$) (Fig. 4g). These results indicate that Mat administration reduced the Aβ plaques and Aβ oligomers in vivo.

Mat Weakens the RAGE Signaling Pathway and Proinflammatory Cytokines in APP/PS1 Transgenic Mice

We also analyzed the levels of proteins that were associated with the RAGE signaling pathway, APP, BACE1, and NF-kB in the Mat-treated AD mouse model. As shown in Fig. 5a, western blotting analysis showed that the APP expression level was not influenced by Mat ($p = 0.471$) (Fig. 5a), whereas the protein levels of NF-kB and BACE1 in the Mat-treated mice were significantly lower than those in the control AD mice ($p = 0.0364$ and $p = 0.0198$, respectively) (Fig. 5b, c). Moreover, ELISA analysis indicated that the proinflammatory cytokines TNF-α and IL-1β were downregulated in the Mat-treated group ($p = 0.0157$ and $p = 0.0122$, respectively) (Fig. 5d, e), which is consistent with the trend of the expression levels of NF-κB. These results suggested that Mat downregulated the RAGE signaling pathway and ultimately delayed the inflammatory process in AD mouse model. In addition, we detected the concentration of Mat in the brains of mice with the administration of high dose of Mat over a period of time (0.5, 1, 2, and 4 h), and the HPLC assay demonstrated that an effective concentration of Mat was found in the brain of Mat-treated mouse in 1 h, suggesting that the high dose of Mat administration could be transported through the BBB (Fig. 5f).

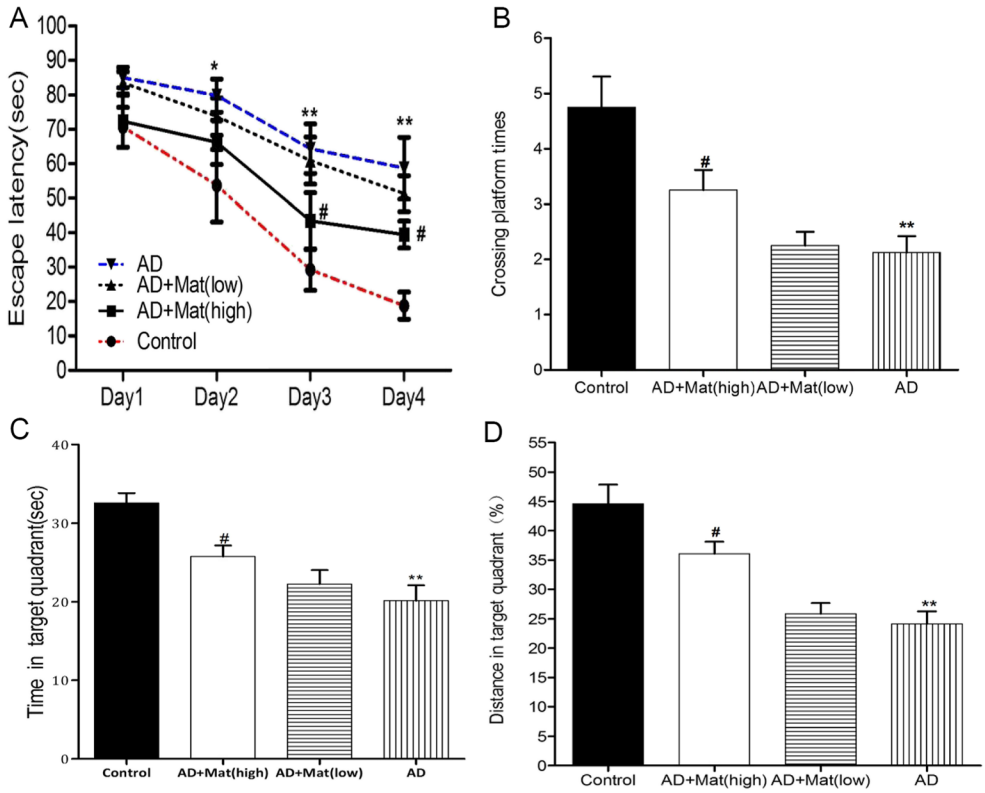

Fig. 3 Mat attenuates the memory deficits of the AD transgenic mice. MWM tests were performed to evaluate learning and memory in an AD mouse model. The mice in each group were given four training trials per day for four consecutive days to locate and climb onto the hidden platform. **a** The influence of Mat on swimming times during the training test; the mean escape latency reflects every group that was trained to find the platform that was placed in a fixed location in the pool. **b** The influence of Mat on the number platform crossings during the learning sessions. **c** The influence of Mat on the percentage of the total distance spent in the target quadrant. **d** The influence of Mat on the time spent in the target quadrant. The data are the mean ± SEM. $*p < 0.05$ and $**p < 0.01$, versus the control wild-type mice; $\#p < 0.05$ versus the control APP/PS1 transgenic mice

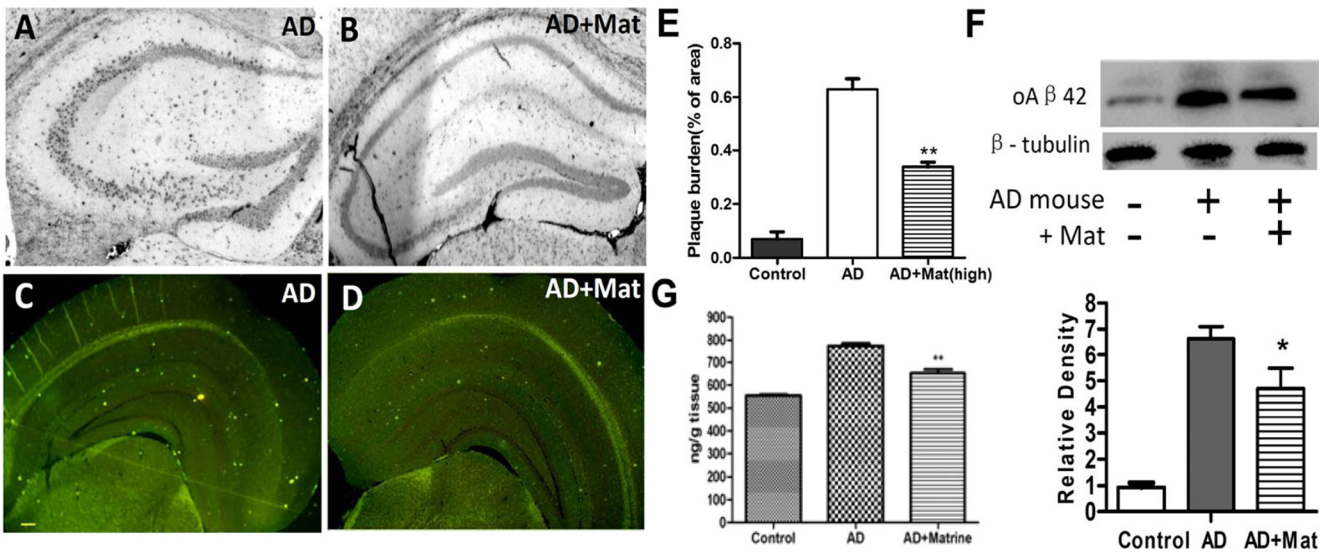

Fig. 4 Mat reduced Aβ levels in the hippocampus of the APP/PS1 transgenic mice. **a**, **b** The immunohistochemistry assay showed the Aβ plaques in hippocampus in the control/ high dose Mat-treated AD mice. **c**, **d** The immunofluorescence assay showed the Aβ plaques of brain in the control/ high dose Mat-treated AD mice. **e** The relative plaque burden area assay showed that Mat reduced Aβ plaques by 53.89 % compared to the control AD mouse model. **f** Western blotting assay showed expression levels of oAβ in the hippocampus of the high-dose Mat-treated/control AD mice. **g** ELISA assay showed the levels of soluble Aβ in high dose Mat-treated/control AD mice. The data are mean ± SEM. $*p < 0.05$ and $**p < 0.01$, versus the control AD mice model

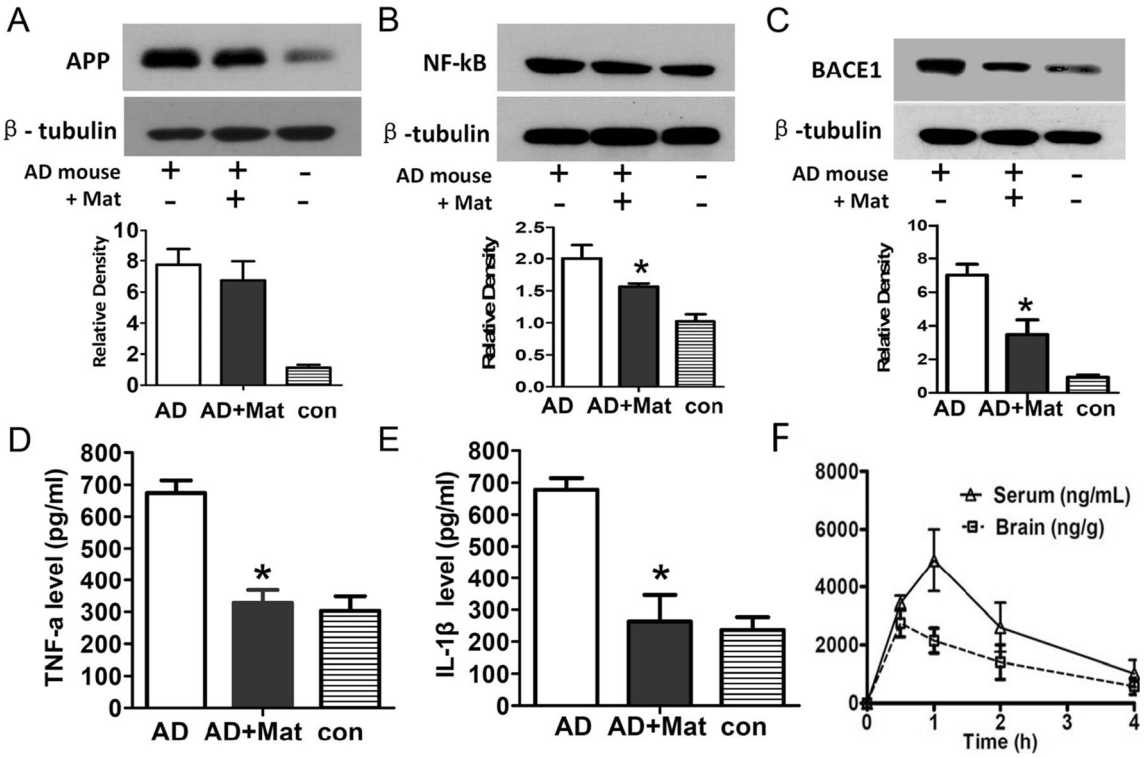

Fig. 5 The effect of Mat treatment on the expression levels of APP, BACE1, NF-κB, and the proinflammatory factors IL-1β and TNF-α in the AD mouse model. **a**–**c** Western blotting assays showed the protein expression levels of APP (**a**), BACE1 (**b**), and NF-κB (**c**) in the hippocampus of the high-dose Mat-treated/control AD mice. **d**, **e** ELISA assay showed the expression levels of TNF-α (**d**) and IL-1β (**e**) in the hippocampus of the Mat-treated AD mice. **f** HPLC assay was performed on the brain and serum samples from the BALB/c mice which administered the high dose of Mat. The data are the mean ± SEM; $*p < 0.05$, versus the control AD mouse model

Molecular Docking Analysis Predicts Interactions between Mat and the Two Target Proteins: Aβ42 Monomers and RAGE

Molecular docking analysis between Mat and the two target proteins, Aβ42 monomers and RAGE, was preformed to predict whether Mat interacted directly with the two targets and explored the molecular mechanism underlying this effect. The small molecule Mat (Fig. 6a, b) was constructed and solvated, energy was minimized, and the potential energy of the molecular system dropped to a stable level which was consistent with previous research (Fig. 6c) [44]. As shown in Fig. 6e, f, the major interaction were found in the middle region of the Aβ42 monomer (Fig. 6f, residues 14–30 were colored cyan) which were stabilized mainly by Van Edward force, the total interaction energy was −8.69 kcal/mol. For the docking analysis between Mat and the other target RAGE, we choose the Crystal structure of RAGE V domain which has been reported as the ligand binding region of RAGE [45, 46]. Considering that Mat is a small hydrophobic molecule, three regions for potential for Mat binding were found in the V domain of RAGE (Fig. 6g), zone 1 with the positive charge-rich region, and zone 2 and zone 3 with the hydrophobic region (green area, orange area, and pink area in Fig. 6g, respectively), and the docking analysis showed that Mat has no significant interaction with zone 1 and zone 2; however, a strong interaction was found in zone 3 (−38.96 kcal/mol). As shown in Fig. 6h, hydrogen bonds were formed between the carbonyl of Mat and amide group of Lys37, with the further analysis, and we confirmed that besides the hydrogen bonding interaction between Mat and Lys37 (-14.51 kcal/mol), Val35, Leu36, leu34, and Ile26 contribute to the stable interaction through the hydrophobic interaction (7.07, 4.70, 2.38, and 2.19 kcal/mol, respectively). Based on the above data, we speculate that Mat may downregulate the Aβ/RAGE signal pathway through block the binding between RAGE V domain and ligands.

Discussion

The treatment of AD is a topic that has puzzled researchers for many years as the currently used drugs, which target AChE or NMDA receptors, can only improve the symptoms of AD and cannot reverse or even delay the development of AD. Accordingly, new strategies are needed for more effective treatment of AD. Though controversial, the current mainstream theory still considers Aβ the most important target for the cure of AD. In this study, we sought to identify a compound that could delay the pathological process of AD

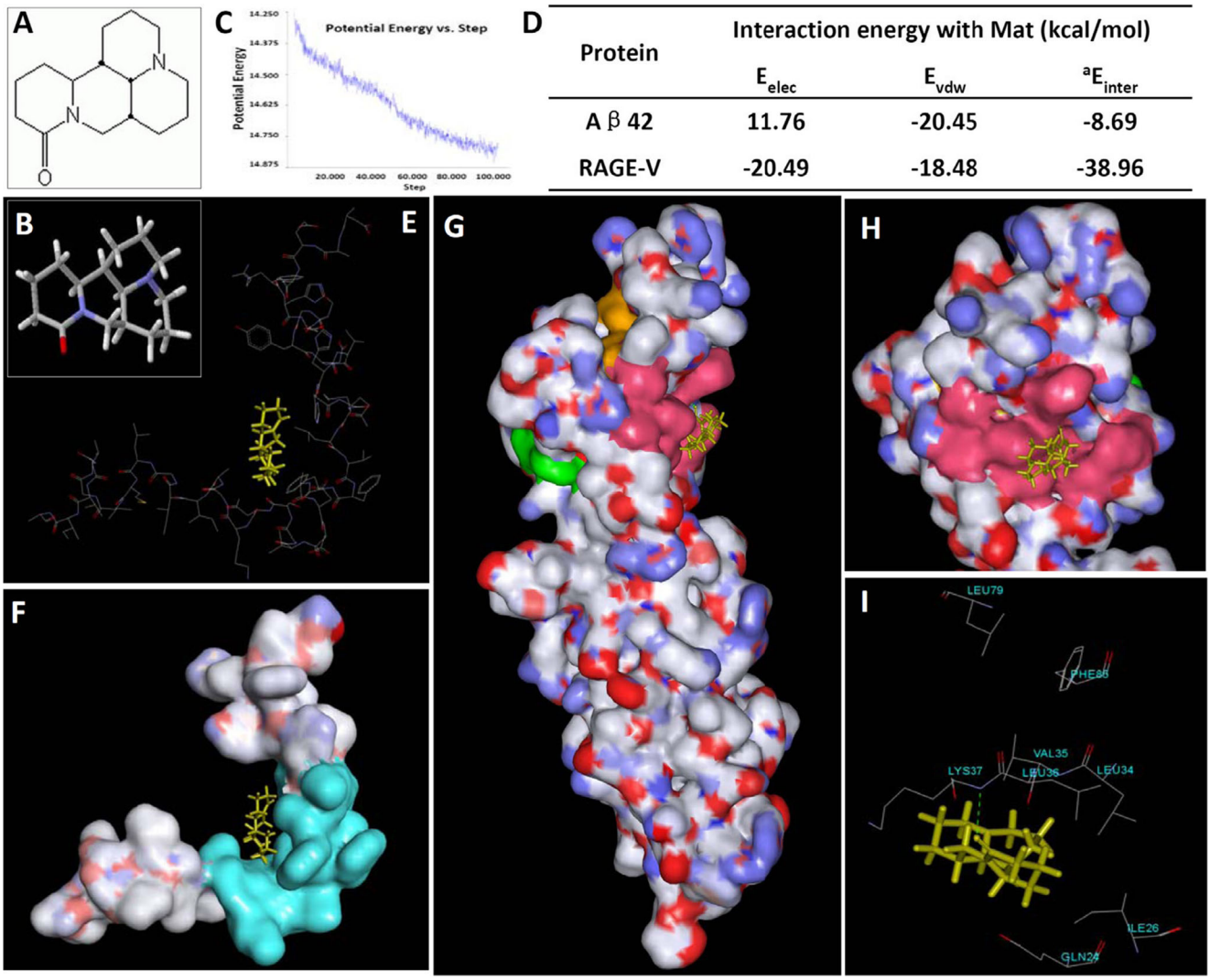

Protein	Interaction energy with Mat (kcal/mol)		
	E_{elec}	E_{vdw}	$^{a}E_{inter}$
A β 42	11.76	-20.45	-8.69
RAGE-V	-20.49	-18.48	-38.96

Fig. 6 Molecular docking assay between Mat and Aβ42 monomers/RAGE-V domain. **a** The chemical structure of the Mat. **b** The ball-and-stick model of the Mat molecule that was used for the docking simulations. **c** Variation in the potential energy, determined by energy minimization and molecular dynamics simulations for Mat. **d** The main interaction energy between Mat and Aβ42 monomers/RAGE-V domain. **e** Docking complex of Mat with Aβ42 monomer. **f** Molecular surface representation of Aβ42 monomer with mat, residues 14-30 were colored cyan. **g** Docking conformation of RAGE-V domain with Mat, zone 1, zone 2, and zone 3 were colored *green*, *orange*, and *pink*. **h** A close-up of the interaction between RAGE-V domain with mat. **i** Mat and the important residues at zone 3, the names of residue were colored cyan, and the hydrogen bond was colored *green* (color figure online)

through various mechanisms, based on the Aβ hypothesis. Therefore, we attempted to explore multi-target treatment of AD. As the first target, we sought a compound that could attenuate Aβ-induced neurotoxicity by inhibiting Aβ aggregation. When we considered past drug development, the key secretases of the APP pathway were still not clearly progress [47–49]. Therefore, RAGE was chosen as the second therapeutic target in our study due to its close association with the pathological development of AD [29, 31, 35, 36, 38, 50].

The active compounds of 16 traditional Chinese herbal compounds (Cistanche, Epimedium, Acorus gramineus, Poria, Astragalus, fleece-flower root, Rhodiola, Polygala, Gynostemma, Tianma, Angelica, Sophora, Rehmannia, Cnidium fruit, Alpinia oxyphylla Miqand, and Ligustrum lucidum) which have the potential treatment of Alzheimer's disease in Chinese medicine theory were recruited and screened. The screening process was conducted according to the steps and principles as follows: (1) For the consideration of the effective of drug to cross the BBB, the candidate compounds should have the limitation of Molecular Weight (MW) (approximately less than 600) and less hydrogen bond (less than 3); (2) we first screened if the active compounds have significant effect on inhibiting the Aβ-induced neurotoxicity and could disturb the Aβ aggregation; (3) docking analysis was then used to simulate the interaction of the first screened compounds with Aβ42 monomer molecular and RAGE V domain respectively to provide the crucial reference and information of the molecular simulation; and (4) at last

screened candidate compounds were evaluated for the effect on RAGE target in vitro, and the final screened compounds will be evaluated in AD mouse model. Through the screening process, we finally identified a novel candidate drug, Matrine (Mat), which could both inhibit Aβ42-induced cytotoxicity by inhibiting the Aβ42 aggregation and suppress the Aβ/RAGE signaling pathway in vitro, and our in vivo study demonstrated that Mat administration ultimately reduced Aβ levels and chronic inflammation as well as attenuated memory deficits in the APP/PS1 transgenic mice model (Fig. 7).

We believe that inhibiting the aggregation of Aβ is still a viable strategy for the development of drugs for the prevention of AD. Structural analyses of Aβ aggregates have suggested that amino acid residues 13–38 of Aβ42 comprise the main region involved in the formation of Aβ β-strand structure [51–54]. Our docking simulations showed that Mat interacted with Aβ42 mainly through electrostatic interactions and that the optimal conformation of Mat was approximately localized to the 20–33 amino acid residues of the Aβ monomer, which is precisely the area that forms β-sheets. Our ThT fluorescence assay and the TEM-based observations of the aggregation state further confirmed that Mat could inhibit Aβ42 monomer-induced aggregation. Moreover, we also considered that the transition from monomers to oligomers and from oligomers to fibrils could result from different conformational transition processes, however, the crystal structure of the Aβ oligomer remains imperfect as a PDB file. Therefore, we did not speculate about the binding site mediating the Mat-Aβ oligomer interaction in this study. Nevertheless, our in vitro results confirmed that Mat has the ability to inhibit the aggregation of Aβ oligomers, and therefore, the inhibitory effect of Mat ultimately weakened the Aβ-induced cytotoxicity, as expected.

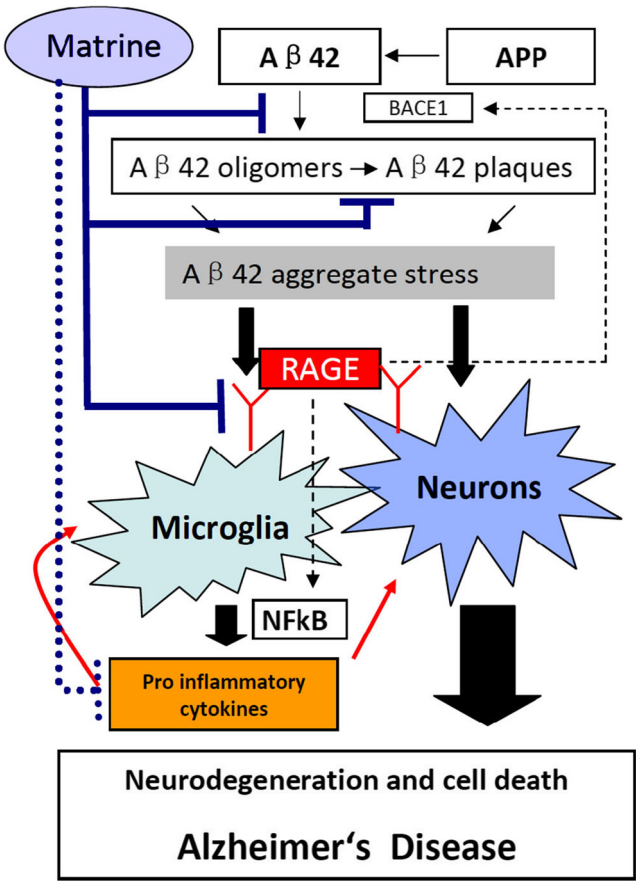

Fig. 7 A simplified schematic illustration of Mat alleviates the development of AD. Mat inhibits the Aβ aggregation, leading to reduce Aβ-induced neurotoxicity. Meanwhile, Mat blocks the ligand binding site of RAGE and weakens the activation of the RAGE pathway with the stimulation of Aβ. Furthermore, the Mat-induced reduction in Aβ levels and chronic inflammation may also contribute to the reduction in the activation of the downstream RAGE signal pathway. In addition, due to the ability of Mat to reduce inflammation, it may also contribute to the anti-inflammatory response, in addition to inhibiting the RAGE signaling pathway. Taken together, the results indicate that Mat is a potential compound with multiple targets that can be used for AD treatment

In recent years, several inhibitors of Aβ aggregation, such as small molecules or peptides, have been reported, while none of these have made substantial progress in clinical trials [55, 56]. This shortcoming led us to consider a more effective strategy for the treatment of AD, wherein a new auxiliary target could have a synergistic effect on Aβ-targeted treatment of AD. Although much remains to be learned, Aβ is known to damage neurons in various ways. For example, secreted Aβ binds to RAGE and mediates pathophysiological cellular responses; this process is thought to be one of the vital pathways of AD [57–59]. Over-activation of the RAGE pathway in AD could trigger the NF-κB signaling pathway and cause the inflammatory response, thereby increasing the levels of proinflammatory cytokines, such as TNF-α and IL-6 [29, 60, 61]. This effect is also accompanied by elevated levels of β-secretase (BACE1) and increased Aβ levels in the brain [29, 30]. Moreover, blocking the RAGE-mediated effects delayed the progression of neurodegeneration and the chronic inflammatory response in a mouse model [62, 63], indicating that regulating or moderately inhibiting the RAGE signaling pathway may have beneficial therapeutic effects in AD. For this reason, we thought that regulating RAGE activity would be more beneficial than blocking it. Our in vitro assays confirmed that Mat could weaken the Aβ-activated RAGE-NF-κB/BACE1 signaling pathways in the RAGE-overexpressing SH-SY5Y cell line. Moreover, the molecular simulations indicated a strong interaction between Mat and a hydrophobic region of the RAGE V1 domain, which is the binding site of the Aβ ligand. Our MST assay further confirmed the interaction between Mat and the RAGE protein. All of these results suggest that Mat may suppress the RAGE signaling pathway by blocking Aβ binding to the RAGE V domain.

Mat is a small, natural molecular compound that is derived from the traditional Chinese herb Sophora flavescens Ait. As one of the main active components of traditional Chinese medicine, it has been used to treat several inflammation-related diseases and also some types of cancer in China. In

particular, several reports have indicated that it has a beneficial, anti-inflammatory effect in different cell lines and cell models of disease [64–68]; however, the mechanism of the anti-inflammatory effect on Mat is still unclear. Our results showed that Mat could inhibit the Aβ-RAGE signal pathway, and as mentioned before, preventing the RAGE signal pathway could delay the inflammatory response. So, we infer that Mat may exert the anti-inflammatory effect through inhibiting the RAGE signal pathway; meanwhile, this may also be one of the mechanisms for its anti-inflammatory effect, it cannot be excluded that Mat may inhibit the inflammatory reaction through the other way in this study and the specific mechanism requires further study.

Some potential limitations of our study should be discussed. First, we are aware that Mat may not be the most effective drug for both targets and that the efficiency and efficacy of its delivery can be improved. Yet, we believe that it was the most suitable compound identified in our first screening based upon our considerations. In further studies, we will try to evaluate more compounds that are based on this core structure but that have been molecularly modified. Second, there are complicated correlations between the two targets in the pathological process of AD. For instance, inhibition of the RAGE pathway consistently reduces Aβ levels and inflammatory responses. Meanwhile, reducing the neurotoxicity of Aβ can also reduce RAGE activation and attenuate chronic inflammation [28, 35, 59, 60] (Fig. 7). Therefore, although we demonstrated that Mat has an effect on the two targets of AD in vitro, it is difficult to evaluate the separate effects on each target or to determine which target of Mat play the more important role in vivo, or even if Mat reduce the chronic inflammation of AD through the other signal pathway, this is the results of a combined effect. Consequently, the in vivo results in this study could confirm that Mat reduced the chronic inflammation and Aβ deposition, and ultimately attenuated the memory deficits of AD transgenic mice, and it could have been caused by the effect of Mat on the above function (Fig. 7). Third, though the in vivo results were statistically significant, the number of the mouse group is relatively not large enough. Anyway, our results demonstrated that Mat could inhibit Aβ42-induced cytotoxicity and suppress the Aβ/RAGE signaling pathway in vitro, and the evaluations in vivo on the effects of Mat are consistent with the in vitro results. And, we believe that this novel multi-target strategy to inhibit Aβ aggregation and block RAGE is worthy of further research. Our future studies will focus on identifying even more effective multi-target compounds for AD treatment based on the molecular structure of Mat.

Acknowledgments Support for this work includes funding from the National Nature Science Foundation of China (81271214, 31171219, and 81401061), the Natural Science Foundation of Guangdong Province (S2013040013740), The key cultivation project of Guangdong Province (4CX14092G), Medical Scientific Research Foundation of Guangdong Province (B2013306), and the Research foundation for the construction of Traditional Chinese medicine of Guangdong Province (20131257).

References

1. Alcolea D, Martinez-Lage P, Sanchez-Juan P, Olazaran J, Antunez C, Izagirre A, Ecay-Torres M, Estanga A et al (2015) Amyloid precursor protein metabolism and inflammation markers in preclinical Alzheimer disease. Neurology 85(7):626–633. doi:10.1212/WNL.0000000000001859
2. Dal Pra I, Chiarini A, Pacchiana R, Chakravarthy B, Whitfield JF, Armato U (2008) Emerging concepts of how beta-amyloid proteins and pro-inflammatory cytokines might collaborate to produce an 'Alzheimer brain' (Review). Mol Med Rep 1(2):173–178
3. Bloom GS (2014) Amyloid-beta and tau: the trigger and bullet in Alzheimer disease pathogenesis. JAMA Neurol 71(4):505–508. doi:10.1001/jamaneurol.2013.5847
4. Chetelat G (2013) Alzheimer disease: Abeta-independent processes-rethinking preclinical AD. Nat Rev Neurol 9(3):123–124. doi:10.1038/nrneurol.2013.21
5. Nixon RA (2014) Alzheimer neurodegeneration, autophagy, and Abeta secretion: the ins and outs (comment on DOI 10.1002/bies.201400002). Bioessays 36(6):547. doi:10.1002/bies.201400064
6. Clarke JR, Lyra ESNM, Figueiredo CP, Frozza RL, Ledo JH, Beckman D, Katashima CK, Razolli D et al (2015) Alzheimer-associated Abeta oligomers impact the central nervous system to induce peripheral metabolic deregulation. EMBO Mol Med 7(2):190–210. doi:10.15252/emmm.201404183
7. Cheng IH, Scearce-Levie K, Legleiter J, Palop JJ, Gerstein H, Bien-Ly N, Puolivali J, Lesne S et al (2007) Accelerating amyloid-beta fibrillization reduces oligomer levels and functional deficits in Alzheimer disease mouse models. J Biol Chem 282(33):23818–23828. doi:10.1074/jbc.M701078200
8. Yu X, Wang Q, Pan Q, Zhou F, Zheng J (2013) Molecular interactions of Alzheimer amyloid-beta oligomers with neutral and negatively charged lipid bilayers. Phys Chem Chem Phys 15(23):8878–8889. doi:10.1039/c3cp44448a
9. Morohashi Y, Tomita T, Iwatsubo T (2010) Molecular targeted therapy in Alzheimer disease. Nihon Rinsho 68(10):1906–1910
10. Miners JS, Barua N, Kehoe PG, Gill S, Love S (2011) Abeta-degrading enzymes: potential for treatment of Alzheimer disease. J Neuropathol Exp Neurol 70(11):944–959. doi:10.1097/NEN.0b013e3182345e46
11. Lemere CA, Maier M, Jiang L, Peng Y, Seabrook TJ (2006) Amyloid-beta immunotherapy for the prevention and treatment of Alzheimer disease: lessons from mice, monkeys, and humans. Rejuvenation Res 9(1):77–84. doi:10.1089/rej.2006.9.77
12. Estrada LD, Soto C (2007) Disrupting beta-amyloid aggregation for Alzheimer disease treatment. Curr Top Med Chem 7(1):115–126
13. Fang L, Gou S, Liu X, Cao F, Cheng L (2014) Design, synthesis and anti-Alzheimer properties of dimethylaminomethyl-substituted curcumin derivatives. Bioorg Med Chem Lett 24(1):40–43. doi:10.1016/j.bmcl.2013.12.011
14. Garcia-Alloza M, Borrelli LA, Rozkalne A, Hyman BT, Bacskai BJ (2007) Curcumin labels amyloid pathology in vivo, disrupts existing plaques, and partially restores distorted neurites in an Alzheimer mouse model. J Neurochem 102(4):1095–1104. doi:10.1111/j.1471-4159.2007.04613.x
15. McKoy AF, Chen J, Schupbach T, Hecht MH (2012) A novel inhibitor of amyloid beta (Abeta) peptide aggregation: from high

throughput screening to efficacy in an animal model of Alzheimer disease. J Biol Chem 287(46):38992–39000. doi:10.1074/jbc.M112.348037
16. Lai AY, McLaurin J (2012) Inhibition of amyloid-beta peptide aggregation rescues the autophagic deficits in the TgCRND8 mouse model of Alzheimer disease. Biochim Biophys Acta 1822(10): 1629–1637. doi:10.1016/j.bbadis.2012.07.003
17. Hamada Y, Miyamoto N, Kiso Y (2015) Novel beta-amyloid aggregation inhibitors possessing a turn mimic. Bioorg Med Chem Lett 25(7):1572–1576. doi:10.1016/j.bmcl.2015.02.016
18. Peters C, Fernandez-Perez EJ, Burgos CF, Espinoza MP, Castillo C, Urrutia JC, Streltsov VA, Opazo C et al (2013) Inhibition of amyloid beta-induced synaptotoxicity by a pentapeptide derived from the glycine zipper region of the neurotoxic peptide. Neurobiol Aging 34(12):2805–2814. doi:10.1016/j.neurobiolaging.2013.06.001
19. Jiang P, Li W, Shea JE, Mu Y (2011) Resveratrol inhibits the formation of multiple-layered beta-sheet oligomers of the human islet amyloid polypeptide segment 22-27. Biophys J 100(6):1550–1558. doi:10.1016/j.bpj.2011.02.010
20. Fukumoto H, Takahashi H, Tarui N, Matsui J, Tomita T, Hirode M, Sagayama M, Maeda R et al (2010) A noncompetitive BACE1 inhibitor TAK-070 ameliorates Abeta pathology and behavioral deficits in a mouse model of Alzheimer's disease. J Neurosci 30(33):11157–11166. doi:10.1523/JNEUROSCI.2884-10.2010
21. Huang HJ, Lee CC, Chen CY (2014) In silico design of BACE1 inhibitor for Alzheimer's disease by traditional Chinese medicine. Biomed Res Int 2014:741703. doi:10.1155/2014/741703
22. Cheng X, Zhou Y, Gu W, Wu J, Nie A, Cheng J, Zhou J, Zhou W et al (2013) The selective BACE1 inhibitor VIa reduces amyloid-beta production in cell and mouse models of Alzheimer's disease. J Alzheimers Dis 37(4):823–834. doi:10.3233/JAD-130836
23. Meunier J, Villard V, Givalois L, Maurice T (2013) The gamma-secretase inhibitor 2-[(1R)-1-[(4-chlorophenyl)sulfonyl](2,5-difluorophenyl) amino]ethyl-5-fluorobenzenebutanoic acid (BMS-299897) alleviates Abeta1-42 seeding and short-term memory deficits in the Abeta25-35 mouse model of Alzheimer's disease. Eur J Pharmacol 698(1-3):193–199. doi:10.1016/j.ejphar.2012.10.033
24. Mori T, Rezai-Zadeh K, Koyama N, Arendash GW, Yamaguchi H, Kakuda N, Horikoshi-Sakuraba Y, Tan J et al (2012) Tannic acid is a natural beta-secretase inhibitor that prevents cognitive impairment and mitigates Alzheimer-like pathology in transgenic mice. J Biol Chem 287(9):6912–6927. doi:10.1074/jbc.M111.294025
25. Rafii MS, Aisen PS (2015) Advances in Alzheimer's disease drug development. BMC Med 13:62. doi:10.1186/s12916-015-0297-4
26. Liu H, Wang L, Su W, Xie XQ (2014) Advances in recent patent and clinical trial drug development for Alzheimer's disease. Pharm Pat Anal 3(4):429–447. doi:10.4155/ppa.14.22
27. Yan SD, Chen X, Fu J, Chen M, Zhu H, Roher A, Slattery T, Zhao L et al (1996) RAGE and amyloid-beta peptide neurotoxicity in Alzheimer's disease. Nature 382(6593):685–691. doi:10.1038/382685a0
28. Schmidt AM, Sahagan B, Nelson RB, Selmer J, Rothlein R, Bell JM (2009) The role of RAGE in amyloid-beta peptide-mediated pathology in Alzheimer's disease. Curr Opin Investig Drugs 10(7):672–680
29. Guglielmotto M, Aragno M, Tamagno E, Vercellinatto I, Visentin S, Medana C, Catalano MG, Smith MA et al (2012) AGEs/RAGE complex upregulates BACE1 via NF-kappaB pathway activation. Neurobiol Aging 33(1):196. doi:10.1016/j.neurobiolaging.2010.05.026
30. Cho HJ, Son SM, Jin SM, Hong HS, Shin DH, Kim SJ, Huh K, Mook-Jung I (2009) RAGE regulates BACE1 and Abeta generation via NFAT1 activation in Alzheimer's disease animal model. FASEB J 23(8):2639–2649. doi:10.1096/fj.08-126383
31. Miller MC, Tavares R, Johanson CE, Hovanesian V, Donahue JE, Gonzalez L, Silverberg GD, Stopa EG (2008) Hippocampal RAGE immunoreactivity in early and advanced Alzheimer's disease. Brain Res 1230:273–280. doi:10.1016/j.brainres.2008.06.124
32. Slowik A, Merres J, Elfgen A, Jansen S, Mohr F, Wruck CJ, Pufe T, Brandenburg LO (2012) Involvement of formyl peptide receptors in receptor for advanced glycation end products (RAGE)–and amyloid beta 1-42-induced signal transduction in glial cells. Mol Neurodegener 7:55. doi:10.1186/1750-1326-7-55
33. Deane R, Du Yan S, Submamaryan RK, LaRue B, Jovanovic S, Hogg E, Welch D, Manness L et al (2003) RAGE mediates amyloid-beta peptide transport across the blood-brain barrier and accumulation in brain. Nat Med 9(7):907–913. doi:10.1038/nm890
34. Perrone L, Sbai O, Nawroth PP, Bierhaus A (2012) The complexity of sporadic Alzheimer's Disease pathogenesis: the role of RAGE as therapeutic target to promote neuroprotection by inhibiting neurovascular dysfunction. Int J Alzheimers Dis 2012:734956. doi:10.1155/2012/734956
35. Galasko D, Bell J, Mancuso JY, Kupiec JW, Sabbagh MN, van Dyck C, Thomas RG, Aisen PS (2014) Clinical trial of an inhibitor of RAGE-Abeta interactions in Alzheimer disease. Neurology 82(17):1536–1542. doi:10.1212/WNL.0000000000000364
36. Deane R, Singh I, Sagare AP, Bell RD, Ross NT, LaRue B, Love R, Perry S et al (2012) A multimodal RAGE-specific inhibitor reduces amyloid beta-mediated brain disorder in a mouse model of Alzheimer disease. J Clin Invest 122(4): 1377–1392. doi:10.1172/JCI58642
37. Sabbagh MN, Agro A, Bell J, Aisen PS, Schweizer E, Galasko D (2011) PF-04494700, an oral inhibitor of receptor for advanced glycation end products (RAGE), in Alzheimer disease. Alzheimer Dis Assoc Disord 25(3):206–212. doi:10.1097/WAD.0b013e318204b550
38. Matrone C, Djelloul M, Taglialatela G, Perrone L (2015) Inflammatory risk factors and pathologies promoting Alzheimer's disease progression: is RAGE the key? Histol Histopathol 30(2): 125–139, HH-11-519
39. Viayna E, Sabate R, Munoz-Torrero D (2013) Dual inhibitors of beta-amyloid aggregation and acetylcholinesterase as multi-target anti-Alzheimer drug candidates. Curr Top Med Chem 13(15): 1820–1842, 54933
40. Sivilia S, Lorenzini L, Giuliani A, Gusciglio M, Fernandez M, Baldassarro VA, Mangano C, Ferraro L et al (2013) Multi-target action of the novel anti-Alzheimer compound CHF5074: in vivo study of long term treatment in Tg2576 mice. BMC Neurosci 14: 44. doi:10.1186/1471-2202-14-44
41. Parker JL, Newstead S (2014) Molecular basis of nitrate uptake by the plant nitrate transporter NRT1.1. Nature 507(7490):68–72. doi:10.1038/nature13116
42. Xiong X, Coombs PJ, Martin SR, Liu J, Xiao H, McCauley JW, Locher K, Walker PA et al (2013) Receptor binding by a ferret-transmissible H5 avian influenza virus. Nature 497(7449):392–396. doi:10.1038/nature12144
43. Cao H, Gao G, Gu Y, Zhang J, Zhang Y (2014) Trp358 is a key residue for the multiple catalytic activities of multifunctional amylase OPMA-N from Bacillus sp. ZW2531-1. Appl Microbiol Biotechnol 98(5):2101–2111. doi:10.1007/s00253-013-5085-5
44. Cui L, Zhang Y, Cao H, Wang Y, Teng T, Ma G, Li Y, Li K (2013) Ferulic acid inhibits the transition of amyloid-beta42 monomers to oligomers but accelerates the transition from oligomers to fibrils. J Alzheimers Dis 37(1):19–28. doi:10.3233/JAD-130164
45. Chaney MO, Stine WB, Kokjohn TA, Kuo YM, Esh C, Rahman A, Luehrs DC, Schmidt AM et al (2005) RAGE and amyloid beta interactions: atomic force microscopy and molecular modeling. Biochim Biophys Acta 1741(1-2):199–205. doi:10.1016/j.bbadis.2005.03.014
46. Park H, Adsit FG, Boyington JC (2010) The 1.5 A crystal structure of human receptor for advanced glycation endproducts (RAGE)

ectodomains reveals unique features determining ligand binding. J Biol Chem 285(52):40762–40770. doi:10.1074/jbc.M110.169276
47. De Strooper B (2014) Lessons from a failed gamma-secretase Alzheimer trial. Cell 159(4):721–726. doi:10.1016/j.cell.2014.10.016
48. Tang J, Ghosh A (2011) Treating transgenic Alzheimer mice with a beta-secretase inhibitor, what have we learned? Aging (Albany NY) 3(1):14–16, 100267
49. Ziani-Cherif C, Mostefa-Kara B, Brixi-Gormat FZ (2006) Gamma-secretase as a pharmacological target in Alzheimer disease research: when, why and how? Curr Pharm Des 12(33):4313–4335
50. Deane RJ (2012) Is RAGE still a therapeutic target for Alzheimer's disease? Future Med Chem 4(7):915–925. doi:10.4155/fmc.12.51
51. McKoy AF, Chen J, Schupbach T, Hecht MH (2014) Structure-activity relationships for a series of compounds that inhibit aggregation of the Alzheimer's peptide, Abeta42. Chem Biol Drug Des 84(5):505–512. doi:10.1111/cbdd.12341
52. Ahmed M, Davis J, Aucoin D, Sato T, Ahuja S, Aimoto S, Elliott JI, Van Nostrand WE et al (2010) Structural conversion of neurotoxic amyloid-beta(1-42) oligomers to fibrils. Nat Struct Mol Biol 17(5):561–567. doi:10.1038/nsmb.1799
53. Naldi M, Fiori J, Pistolozzi M, Drake AF, Bertucci C, Wu R, Mlynarczyk K, Filipek S et al (2012) Amyloid beta-peptide 25-35 self-assembly and its inhibition: a model undecapeptide system to gain atomistic and secondary structure details of the Alzheimer's disease process and treatment. ACS Chem Neurosci 3(11):952–962. doi:10.1021/cn3000982
54. Davis CH, Berkowitz ML (2009) Structure of the amyloid-beta (1-42) monomer absorbed to model phospholipid bilayers: a molecular dynamics study. J Phys Chem B 113(43):14480–14486. doi:10.1021/jp905889z
55. Schneider LS, Mangialasche F, Andreasen N, Feldman H, Giacobini E, Jones R, Mantua V, Mecocci P et al (2014) Clinical trials and late-stage drug development for Alzheimer's disease: an appraisal from 1984 to 2014. J Intern Med 275(3):251–283. doi:10.1111/joim.12191
56. Mangialasche F, Solomon A, Winblad B, Mecocci P, Kivipelto M (2010) Alzheimer's disease: clinical trials and drug development. Lancet Neurol 9(7):702–716. doi:10.1016/S1474-4422(10)70119-8
57. Chen X, Walker DG, Schmidt AM, Arancio O, Lue LF, Yan SD (2007) RAGE: a potential target for Abeta-mediated cellular perturbation in Alzheimer's disease. Curr Mol Med 7(8):735–742
58. Yan SD, Stern D, Kane MD, Kuo YM, Lampert HC, Roher AE (1998) RAGE-Abeta interactions in the pathophysiology of Alzheimer's disease. Restor Neurol Neurosci 12(2-3):167–173
59. Yan SS, Chen D, Yan S, Guo L, Du H, Chen JX (2012) RAGE is a key cellular target for Abeta-induced perturbation in Alzheimer's disease. Front Biosci (Schol Ed) 4:240–250, 265
60. Fang F, Lue LF, Yan S, Xu H, Luddy JS, Chen D, Walker DG, Stern DM et al (2010) RAGE-dependent signaling in microglia contributes to neuroinflammation, Abeta accumulation, and impaired learning/memory in a mouse model of Alzheimer's disease. FASEB J 24(4):1043–1055. doi:10.1096/fj.09-139634
61. Onyango IG, Tuttle JB, Bennett JP Jr (2005) Altered intracellular signaling and reduced viability of Alzheimer's disease neuronal cybrids is reproduced by beta-amyloid peptide acting through receptor for advanced glycation end products (RAGE). Mol Cell Neurosci 29(2):333–343. doi:10.1016/j.mcn.2005.02.012
62. Takuma K, Fang F, Zhang W, Yan S, Fukuzaki E, Du H, Sosunov A, McKhann G et al (2009) RAGE-mediated signaling contributes to intraneuronal transport of amyloid-beta and neuronal dysfunction. Proc Natl Acad Sci U S A 106(47):20021–20026. doi:10.1073/pnas.0905686106
63. Yan SF, Ramasamy R, Schmidt AM (2010) Soluble RAGE: therapy and biomarker in unraveling the RAGE axis in chronic disease and aging. Biochem Pharmacol 79(10):1379–1386. doi:10.1016/j.bcp.2010.01.013
64. Kan QC, Lv P, Zhang XJ, Xu YM, Zhang GX, Zhu L (2015) Matrine protects neuro-axon from CNS inflammation-induced injury. Exp Mol Pathol 98(1):124–130. doi:10.1016/j.yexmp.2015.01.001
65. Chuang CY, Xiao JG, Chiou GC (1987) Ocular anti-inflammatory actions of matrine. J Ocul Pharmacol 3(2):129–134
66. Zhang B, Liu ZY, Li YY, Luo Y, Liu ML, Dong HY, Wang YX, Liu Y et al (2011) Antiinflammatory effects of matrine in LPS-induced acute lung injury in mice. Eur J Pharm Sci 44(5):573–579. doi:10.1016/j.ejps.2011.09.020
67. Liu N, Kan QC, Zhang XJ, Xv YM, Zhang S, Zhang GX, Zhu L (2014) Upregulation of immunomodulatory molecules by matrine treatment in experimental autoimmune encephalomyelitis. Exp Mol Pathol 97(3):470–476. doi:10.1016/j.yexmp.2014.10.004
68. Suo Z, Liu Y, Ferreri M, Zhang T, Liu Z, Mu X, Han B (2009) Impact of matrine on inflammation related factors in rat intestinal microvascular endothelial cells. J Ethnopharmacol 125(3):404–409. doi:10.1016/j.jep.2009.07.023